MATHEMATICAL MODELING AND COMPUTING, Vol. 11, No. 3, pp. 682–691 (2024)

Towards a Nash game strategy approach to blind image deconvolution: a fractional-order derivative variational framework

Salah F.-E.[1], Moussaid N.[1], Abassi A.[1], Jadir A.[2]

[1]*LMCSA, FSTM, Hassan II University of Casablanca, Mohammedia, Morocco*
[2]*FSTG, Cadi Ayyad University, Marrakech, Morocco*

(Received 3 December 2023; Revised 19 July 2024; Accepted 22 July 2024)

Image restoration is a critical process aimed at recovering degraded images, often impacted by factors including motion blur, sensor blurring, defocused photography, optical aberrations, atmospheric distortions, and noise-induced blur. The inherent challenge lies in the typical scenario where both the original image and the blur kernel (Point Spread Function, PSF) are unknown. This restorative process finds applications in various fields, including sensing, medical imaging, astronomy, remote sensing, and criminal investigations. This paper introduces an innovative approach to blind image deconvolution based on Nash game theory. Our focus is placed on restoring linearly corrupted images without processing explicit knowledge of the original image or the blur kernel (PSF). The proposed method formulates blind deconvolution as a two-player static game, with one player dedicated to image deblurring and the other focused on estimating the PSF. The optimal solution is characterized as Nash equilibrium, resulting in effective image restoration. Moreover, we present an enhanced game formulation that incorporates fractional-order derivatives. This unique extension has the potential to improve image restoration accuracy and resilience, leading to breakthroughs in blind image deconvolution and practical applications.

Keywords: *blind deconvolution; restoration; multi-criteria optimization; fractional-order derivative; Nash equilibrium.*

2010 MSC: 90C29, 91A05, 58E17, 65K10 **DOI:** 10.23939/mmc2024.03.682

1. Introduction

Image processing assumes a crucial role across diverse fields, and at its core lies the essential task of image restoration [1–3]. This encompasses a spectrum of techniques dedicated to enhancing the quality of degraded or blurred digital images by recovering their latent or pristine forms, even when confronted with unknown factors such as the point spread function (PSF) and the original image. These degradations can originate from a variety of sources, including sensor and motion blur, defocused camera settings, or atmospheric distortions.

In specific applications, the blurring process lacks a well-defined description and necessitates reconstruction alongside the image. In these scenarios, terms like deblurring, deconvolution, or image restoration can be used interchangeably to convey the objective of restoring clarity and fidelity to the visual content.

We model the blurred image $b(x, y)$ as

$$b(x, y) = [\kappa \circledast v](x, y) + \eta(x, y), \tag{1}$$

where b represents the observed (blurry and noisy) image, κ is the point spread function (PSF), $\circledast$ denotes the operation of deconvolution, v represents the sharp unknown image. Moreover, η denotes an unspecified form of noise introduced into the blurred image.

Given the ill-posed nature of the problem at hand, it is pertinent to note that numerous regularized image restoration methods, taking advantages of previous research, have been extensively developed to mitigate these challenges. These methods can be outlined as follows:

$$\min_v \psi(v) + \frac{\alpha}{2}\|\kappa \circledast v - b\|_2^2, \tag{2}$$

where:

- the fidelity term $\|\kappa \circledast v - b\|_2^2$ measures, in an appropriate sense, the distance between the data b and its reconstruction v;
- the regularization term $\psi(v)$ plays a significant role in the reconstruction process by incorporating a priori knowledge about the image being reconstructed. It involves imposing regularity on it. This is typically done by incorporating some norms of the image gradient in imaging application. In the case of denoising, the regularization term smooths out the noise in the measured image b;
- the weighting parameter $\alpha > 0$ balances the effect of regularization against the fitting of the data. Formula (2) is a general formula for image restoration.

Prominent regularization models encompass Tikhonov regularization, l_1-norm, and TV regularization. Utilizing the total variation regularization method as described in [4], the authors have introduced a blind deconvolution technique for estimating both the Point Spread Function (PSF) and the latent image. This estimation is accomplished through the utilization of a shock filter and the creation of a gradient reliability map. Furthermore, it is worth noting that numerous other works in this field have also harnessed blind deconvolution with total variation regularization like [5–7], demonstrating its effectiveness and versatility.

Osher, Rudin and Fatemi [8], suggested to use total variation regularization, instead of the L^2 one, which leads to the following problem:

$$\min_v J(v) := \frac{1}{2}\|\kappa \circledast v - b\|^2_{L^2(\kappa)} + \alpha \int_\Omega |\nabla v|\, dx. \tag{3}$$

A different method to addressing the blind image deconvolution problem has been presented by Chan and Wong in their paper [9], which involves utilizing the Total Variation (TV) norm instead of H^1 one:

$$\min_{v,\kappa} J(v,\kappa) := \frac{1}{2}\|\kappa * v - b\|^2_{L^2(\Omega)} + \alpha_1 \int_\Omega |\nabla v|\, dx + \alpha_2 \int_\Omega |\nabla \kappa|\, dx. \tag{4}$$

In this context, the positive parameters α_1 and α_2 quantify the balance between achieving a satisfactory fit and ensuring the smoothness of both the solution v and κ, where the total variation TV is defined as

$$\mathrm{TV}(u) := \sup\left\{ \int_\Omega u \operatorname{div} \varphi\, dx \mid \varphi \in \mathcal{C}_0^1 \text{ and } |\varphi|_{L^\infty(\Omega)} \leqslant 1 \right\}. \tag{5}$$

Recent research highlights the significant impact of game theory on image processing tasks. Semmane et al. demonstrated that integrating Nash game theory with machine learning techniques greatly enhances image retrieval performance, achieving more accurate and efficient results [10]. Similarly, Salah and Moussaid applied Nash game theory within machine learning frameworks for similar image retrieval, showing how game-theoretic approaches can effectively optimize retrieval processes [11]. Additionally, the concept of Nash equilibrium has been successfully employed across various image retrieval applications, further proving its effectiveness in improving retrieval outcomes and demonstrating its versatility in the field [12].

Inspired by the last minimization problem (4), another blind deconvolution technique is introduced, solved in Nash game framework. We split the initial optimization variable into two strategies, namely, deblurring and PSF. Subsequently, we formulate a two-player static game of complete information, presenting the following optimization problem:

$$(P1)\colon \begin{cases} J_v(v,\kappa) = \dfrac{1}{2}\|\kappa \circledast v - b\|^2_{L^2(\Omega)} + \alpha \displaystyle\int_\Omega |Dv(x)|\, dx, \\ J_\kappa(v,\kappa) = \dfrac{1}{2}\|\kappa \circledast v - b\|^2_{L^2(\Omega)} + (1-\alpha) \displaystyle\int_\Omega |D\kappa(x)|\, dx, \end{cases} \tag{6}$$

where $\alpha = 2.10^{-6}$. This problem is solved in the framework of Game theory and the solution is defined as Nash equilibrium.

Expanding upon the problem (6), Meskine et al. [13] addressed a generalized form of blind deconvolution problem through the lens of game theory. Specifically, they identified the optimal image and

PSF estimation as a Nash equilibrium. Their approach entailed the minimization of two functionals:

$$(P2)\colon \begin{cases} J_v(v,\kappa) = \dfrac{1}{2}\|\kappa \circledast v - b\|^2_{L^2(\Omega)} + \displaystyle\int_\Omega \alpha(x)|Dv(x)|\,dx, \\ J_\kappa(v,\kappa) = \dfrac{1}{2}\|\kappa \circledast v - b\|^2_{L^2(\Omega)} + \displaystyle\int_\Omega (1-\alpha(x))|D\kappa(x)|\,dx. \end{cases} \tag{7}$$

In the provided expression, $\alpha(x)$ is a function that adapts spatially and with respect to scale. This adaptation is defined as following:

$$\alpha(x) = \frac{1}{1+\lambda|\nabla G_\sigma \circledast b|^2},$$

where $G_\sigma(x) = \frac{1}{2\pi\sigma^2}\exp\big(-\frac{|x|^2}{2\sigma^2}\big)$ represent the Gaussian filter with parameter σ and λ serves as a threshold parameter.

Moreover, advancements in image restoration and contrast enhancement have been achieved through sophisticated mathematical models. For instance, the nonlinear reaction-diffusion model, when paired with a divide-and-conquer strategy, has demonstrated significant improvements in image quality by effectively addressing noise and enhancing details [14]. Additionally, the Gray–Scott model, enhanced with a novel Lattice Boltzmann method, has shown substantial effectiveness in both image restoration and contrast enhancement, providing more refined and accurate results in these applications [15].

Recently, there has been a noteworthy surge of interest in the fractional-order derivative within the engineering field. Serving as a generalization of the traditional integer-order derivative, it has been a focal point of inquiry by eminent mathematicians such as Euler, Hardy, Littlewood, and Liouville [16]. Various formulations of fractional-order derivatives have been proposed, including the Grünwald–Letnikov (G-L) fractional-order derivative, the Cauchy-integral fractional-order derivative (or Riemann–Liouville (R-L) fractional-order derivative), the Caputo fractional-order derivative, and the Fourier domain (frequency domain) definition [17], all of which are frequently employed.

However, the widespread recognition of the significance of fractional-order derivatives took a notable turn with the work of Mandelbrot, who introduced fractals and applied the R-L fractional-order derivative to Brownian motion. Since then, this derivative has garnered substantial attention and found applications in diverse fields. Currently, it has been widely utilized in areas such as noise detection and estimation [18, 19], electromagnetic theory [20], wavelets, splines [21, 22], and various other domains. This growing interest underscores the versatility and potential impact of fractional-order derivatives across a spectrum of engineering applications.

Utilizing the framework of fractional-order derivatives and game theory, we propose in this paper, a new hybrid model formulated as two-players static game. The first player aim is to recover a clean and latent image v by integrating the fractional-order derivative in regularizing it, while the second player has as a mission recovering the PSF function using the second strategy. Two players engage in simultaneous actions until reaching an equilibrium, at each point each player has successfully minimized their respective function, converging upon a shared pair of strategies.

Furthermore, we will employ the widely accepted Grünwald–Letnikov (G-L) fractional-order derivative for implementation. This derivative is acknowledged as an extension of the conventional finite difference of integer orders. Additionally, in order to obtain optimal latent image and PSF function, we solve a multidisciplinary optimization problem from Nash game theory perspective, where we define the solution as Nash equilibrium.

2. Description of the proposed model: formulation of the Nash game

Motivated and inspired by Meskine et al. model, we present in this section a new model of image blind deconvolution and solve it in the Nash game theory and fractional-order derivative variational framework.

2.1. The proposed model

As is common knowledge, the regularization term plays a significant role in the reconstruction process of the image by incorporating a priori knowledge about the image being reconstructed. In the case of denoising, the regularization term smooths out the noise in the measured image.

The fractional-order derivative at a specific point is influenced by the overall characteristics of the entire function, making the fractional-order operator inherently possess non-local properties. This advantageous feature proves beneficial in enhancing texture preservation performance.

The proposed model is defined by replacing the integer derivative of order 1 in the objective function of the first player J_v whose aim is to recover the latent image from the degraded one in model (6), with the fractional-order derivative in the regularization term. The suggested model is formulated as following:

$$(P3)\colon \begin{cases} J_v(v,\kappa) = \dfrac{1}{2}\|\kappa \circledast v - b\|^2_{L^2(\Omega)} + \displaystyle\int_\Omega \alpha(x)|D^\beta v(x)|\,dx, \\ J_\kappa(v,\kappa) = \dfrac{1}{2}\|\kappa \circledast v - b\|^2_{L^2(\Omega)} + \displaystyle\int_\Omega (1-\alpha(x))|D\kappa(x)|\,dx. \end{cases} \tag{8}$$

In this context, $\alpha(x)$ is defined as a spatially and scale-adaptive function, as follows:

$$\alpha(x) = \frac{1}{1+\lambda|\nabla G_\sigma \circledast b|^2},$$

where $G_\sigma(x) = \frac{1}{2\pi\sigma^2}\exp\big(-\frac{|x|^2}{2\sigma^2}\big)$ represents the Gaussian filter with parameter σ, λ represents a threshold parameter, and D^β is the fractional-order derivative of order $\beta \in \{1.2, 1.4, 1.6, 1.8\}$.

Thus, a competitive game formulation emerges as the appropriate resolution of the problem at hand. This work focuses on the challenge of splitting the optimization variable between two players [23]. In the context of this multidisciplinary problem, our focus revolves around two rational players, each driven by distinct objectives. The primary objective for the first player is to minimize the function $J_v(v,\kappa)$, and accordingly, the player adopts the strategy the image intensity, denoted as v. Simultaneously, the second player strives to minimize $J_\kappa(v,\kappa)$ as the secondary objective, selecting PSF as strategy denoted as κ. It is noteworthy that the cost functions $J_v(v,\kappa)$ and $J_\kappa(v,\kappa)$ are contingent upon two coupling domains. Consequently, the strategic choices made by one player exert an influence on the decisions of the other.

The interaction unfolds as a concurrent game, wherein both players strive to minimize their respective objective functions. This dynamic setting persists until a solution is reached, at which point each player achieves their goal with a shared pair of strategies.

2.2. Discretized representations of the fractional-order operators

In this subsection, we outline a discrete representation of the fractional-order derivative following the Grünwald–Letnikov approach. This discretized form extends the methodology used for integral-order derivatives through finite differences, offering enhanced convenience for numerical computations. We have:

$$D^\beta v = \big[D_x^\beta v, D_y^\beta v\big], \quad \beta > 0,$$

where $D_x^\beta v$ and $D_y^\beta v$ denote the derivatives of the image v in the horizontal and vertical directions, respectively, which can be discretized and approximated as

$$D_x^\beta v = \sum_{k=0}^{M-1} (-1)^k C_k^\beta v(x-k, y), \tag{9}$$

$$D_y^\beta v = \sum_{k=0}^{M-1} (-1)^k C_k^\beta v(x, y-k). \tag{10}$$

Here $M \geqslant 3$ is the number of neighboring pixels that are used to approximate the fractional-order derivative at each pixel. The coefficients $\{C_k^\beta\}_{k=0}^{K-1}$ are defined as

$$C_k^\beta = \frac{\Gamma(\beta+1)}{\Gamma(k+1)\Gamma(\beta+1-k)},$$

the Gamma function denoted by $\Gamma(\cdot)$, is expressed as

$$\Gamma(\beta) = \begin{cases} \int_0^\infty x^{\beta-1} dx \ \text{ if } \ \beta > 0, \\ \beta^{-1}\Gamma(\beta+1) \ \text{ if } \ \beta < 0. \end{cases}$$

Remark 1. Typically, the parameter M in the Grünwald–Letnikov fractional-order derivatives (9) and (10) is selected to be greater than 3. Consequently, the fractional-order derivative involves a broader set of pixels compared to the integer-order derivative, which only considers its two or four neighboring pixels. As a result, the fractional-order derivative is inclined to be more advantageous for preserving structures in image restoration.

Theorem 1. *There exists a Nash equilibrium, i.e., a pair of strategies* (v^*, κ^*) *such that*

$$v^* \ \textit{solves} \ \min_v J_v(v, \kappa^*), \tag{11}$$

$$\kappa^* \ \textit{solves} \ \min_\kappa J_\kappa(v^*, \kappa). \tag{12}$$

The existence of an optimal solution for our problem is assured with Theorem 1. The iterative schemes for $J_v(v, \kappa)$ and $J_\kappa(v, \kappa)$ in (8), can be obtained by using their respective first order optimality conditions in the following.

To develop numerical schemes for (11) and (12), we used their first order optimality conditions:

$$\frac{\partial J_v}{\partial v} = \frac{\partial J_\kappa}{\partial \kappa} = 0.$$

Therefore, we formulate an alternating minimization algorithm wherein the function values $J_v(v^m, \kappa^m)$ and $J_\kappa(v^m, \kappa^m)$ consistently decrease with each iteration (as denoted by m). To ensure the derivation of a physically meaningful solution, Chan and Wong [9] imposed the following conditions on v and κ:

$$\int_\Omega \kappa(x, y)\, dx\, dy = 1,$$

$$v(x, y), \kappa(x, y) \geqslant 0,$$

κ is centrosymmetric, i.e.

$$\kappa(x, y) = \kappa(-x, -y).$$

It is noteworthy to emphasize that while the original game under consideration is a non-cooperative static game, computational demands necessitate the exploration of iterative solving methods. In this context, the algorithmic version, Mutual Information Maximization for Input Clustering (MIMICS), transforms the nature of the game into a partially cooperative one. This transformation occurs as two players engage in the exchange of information regarding their respective partial optima throughout the iterative process.

Nash equilibrium algorithm. Determining the optimal values for both v and κ simultaneously is generally a challenging task. A frequently employed technique in such scenarios is alternating minimization, where one variable is updated iteratively while the other is held constant. The computation of the Nash equilibrium is achieved through the following decomposition algorithm.

Algorithm 1 Nash equilibrium Algorithm

Require: An initial strategy $b^{(0)} = (v^{(0)}, \kappa^{(0)})$. Set $m = 0$.

Step 1:

Phase 1: Determine a resolution to the problem $\min_v J_v(v, \kappa^{(m)}) \longrightarrow v^{(m+1)}$.

Phase 2: Determine a resolution to the problem $\min_\kappa J_\kappa(v^{(m)}, \kappa) \longrightarrow \kappa^{(m+1)}$.

Step 2:

Iterate parallel phases 1 and 2, set $b^{(m+1)} = (v^{(m+1)}, \kappa^{(m+1)})$ until we achieve to convergence.

3. Simulation experiments and results analysis

In this section we will test the validity of our approach numerically. To do so we will compare the numerical results obtained by our algorithm using different values of the fractional-order β ($\beta \in \{1.2, 1.4, 1.6, 1.8\}$), with the models (6), (7) and the following predefined methods in MATLAB:

- deconvblind: Blind Deconvolution Algorithm (B-D Algorithm);
- deconvreg: Regularized Filter;
- deconvlucy: Lucy–Richardson Algorithm (L-R Algorithm).

To assess the effectiveness of the restoration outcomes, we employ qualitative measures, specifically the peak signal-to-noise ratio (PSNR) and the structural similarity index measure (SSIM) [24], both widely utilized in image processing. A superior-quality image is characterized by higher PSNR and SSIM values.

In our experiment, we generated the blurred image through convolution with a 5×5 Gaussian kernel of $\sigma = 1$. Additionally, we introduced Gaussian noise with a standard deviation of $V = 0.0001$ to the blurred image.

Moreover, we evaluate the performance of our approach using three color images depicted in Figures 1–3, chosen for simulation purposes. The quality of image restoration results is presented in Tables 1 and 2, respectively.

Table 1. PSNR values for the different models using the test images (bold values indicate the best result).

Image	β values	Our algorithm PSNR	Meskine et al. PSNR	(P1) ($\alpha = 2.10^{-6}$) PSNR	deconvblind PSNR	deconvreg PSNR	deconvlucy PSNR
House	1.2	28.7398	27.6328	27.0856	21.7581	16.6177	21.9817
	1.4	**28.7446**					
	1.6	28.7382					
	1.8	28.7364					
Airplane	1.2	30.2901	28.8182	28.2710	23.7092	17.4771	24.1592
	1.4	30.2812					
	1.6	30.2867					
	1.8	**30.2937**					
Barbara	1.2	28.5052	27.3654	26.8182	25.3688	18.0746	26.1855
	1.4	28.5040					
	1.6	**28.5058**					
	1.8	28.5041					
Peppers	1.2	**29.6390**	28.1503	27.6031	25.1416	17.7496	25.7926
	1.4	29.6388					
	1.6	29.6369					
	1.8	29.6381					

Table 2. SSIM values for the different models using the test images (bold values indicate the best result).

Image	β values	Our algorithm SSIM	Meskine et al. SSIM	(P1) ($\alpha = 2.10^{-6}$) SSIM	deconvblind SSIM	deconvreg SSIM	deconvlucy SSIM
House	1.2	0.9495	0.9429	0.9242	0.9126	0.5964	0.9211
	1.4	**0.9497**					
	1.6	0.9495					
	1.8	0.9495					
Airplane	1.2	0.9011	0.8531	0.8344	0.8858	0.3142	0.8432
	1.4	0.9011					
	1.6	0.9011					
	1.8	**0.9012**					
Barbara	1.2	0.8822	0.8712	0.8525	0.8640	0.5397	0.8835
	1.4	0.8822					
	1.6	**0.8823**					
	1.8	0.8821					
Peppers	1.2	**0.9767**	0.9689	0.9630	0.9639	0.7737	0.9676
	1.4	0.9767					
	1.6	0.9766					
	1.8	0.9767					

The experiments demonstrate that incorporating the fractional-order derivative in the regularization term effectively mitigates the staircase effect, yielding more detailed structures. This improvement is evident in Figures 1–4 when an appropriate order is chosen.

In our specific case, the model utilizing fractional-order derivatives yields superior results compared to the Meskine et al. model and predefined methods in MATLAB.

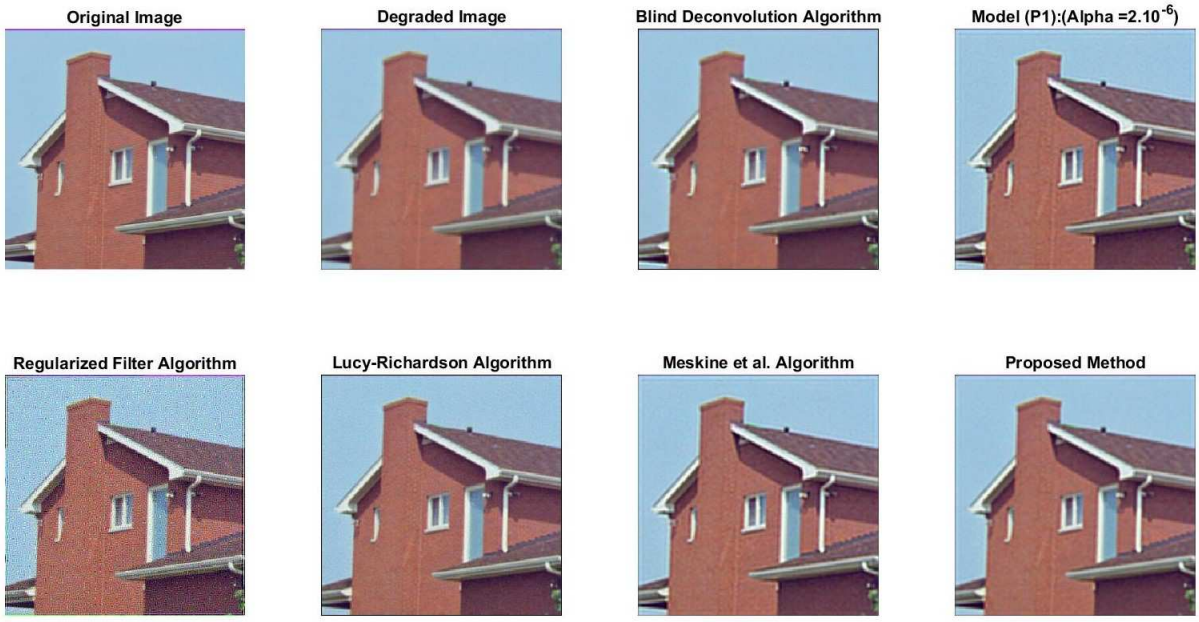

Fig. 1. Comparison of the proposed deconvolution model applied on a blurred House image, with different existing methods: Meskine et al. model, Model (P1) ($\alpha = 2.10^{-6}$), Blind Deconvolution algorithm, Regularized Filter algorithm and Lucy–Richardson algorithm.

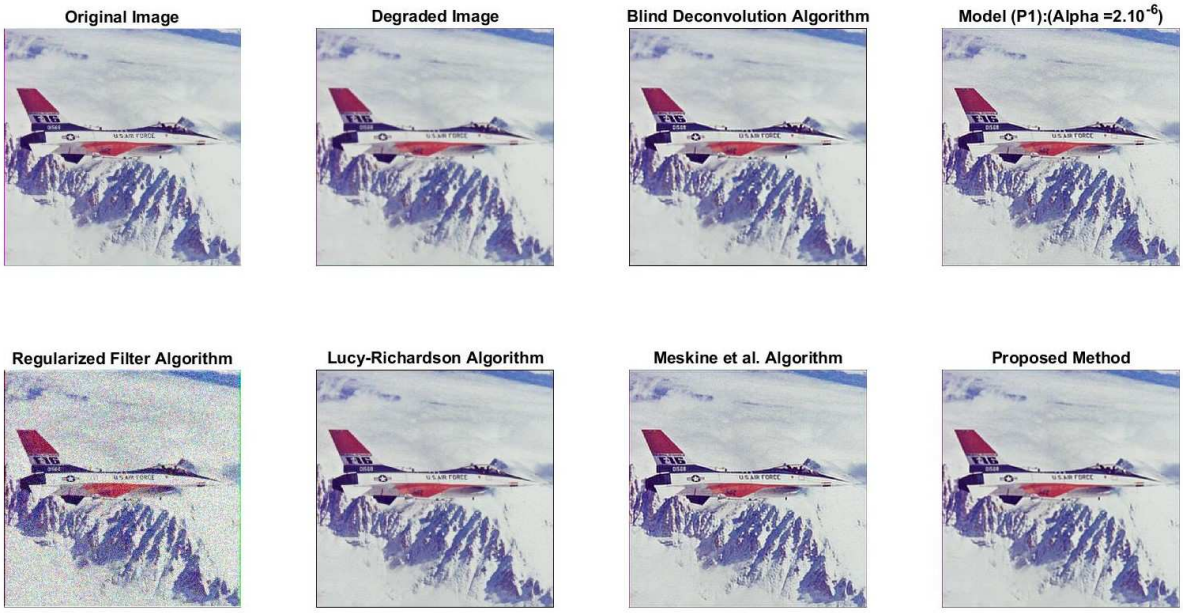

Fig. 2. Comparison of the proposed deconvolution model applied on a blurred Airplane image, with different existing methods: Meskine et al. model, Model (P1) ($\alpha = 2.10^{-6}$), Blind Deconvolution algorithm, Regularized Filter algorithm and Lucy–Richardson algorithm.

The validity of our observations is substantiated by examining the PSNR and SSIM values in Tables 1 and 2, respectively. The proposed model has always highest values compared with the other approaches at each value of the derivatives order.

Meanwhile, in the first test the image House, we notice that the optimal order occurs at $\beta = 1.4$, where test images have the highest PSNR and SSIM values. The second test performed on Airplane image, we have the highest values at the order $\beta = 1.6$, while at the third test we have obtained the highest values of PSNR and SSIM at the order $\beta = 1.8$ and last but not least, we achieved the highest values at the order $\beta = 1.2$.

Fig. 3. Comparison of the proposed deconvolution model applied on a blurred Barbara image, with different existing methods: Meskine et al. model, Model (P1) ($\alpha = 2.10^{-6}$), Blind Deconvolution algorithm, Regularized Filter algorithm and Lucy–Richardson algorithm.

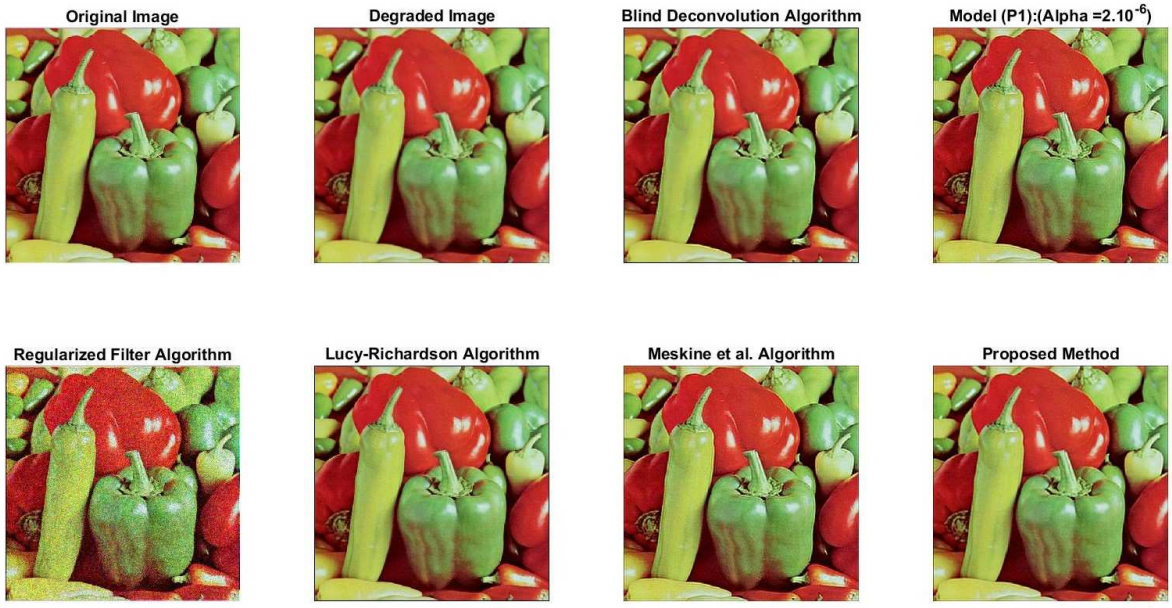

Fig. 4. Comparison of the proposed deconvolution model applied on a blurred Peppers image, with different existing methods: Meskine et al. model, Model (P1) ($\alpha = 2.10^{-6}$), Blind Deconvolution algorithm, Regularized Filter algorithm and Lucy–Richardson algorithm.

4. Conclusion

In this paper, we have successfully introduced a variational model incorporating a fractional-order derivative as a regularizer within the framework of game theory. The experimental outcomes, juxtaposed with those of several relevant models, illustrate the superior performance of our proposed model. Specifically, it demonstrates enhanced efficacy in mitigating the staircase effect during noise removal, as evidenced by both visual and quantitative analyses. Evaluation metrics such as PSNR and SSIM further validate the efficacy of the proposed model.

[1] Ayers G. R., Dainty J. C. Interative blind deconvolution method and its applications. Optics Letters. **13** (7), 547–549 (1988).

[2] Fergus R., Singh B., Hertzmann A., Roweis S. T., Freeman W. T. A removing camerashake from a single photograph. ACM Transactions on Graphics. **25** (3), 787–794 (2006).

[3] Kundur D., Hatzinakos D. Blind image deconvolution. IEEE Signal Processing Magazine. **13** (3), 43–64 (1996).

[4] Liu X. Efficient algorithms for hybrid regularizers based image denoising and deblurring. Computers & Mathematics with Applications. **69** (7), 675–687 (2015).

[5] Ji H., Liu C. Motion blur identification from image gradients. 2008 IEEE Conference on Computer Vision and Pattern Recognition. 1–8 (2008).

[6] Molina R., Mateos J., Katsaggelos A. Blind deconvolution using a variational approach to parameter, image, and blur estimation. IEEE Transactions on Image Processing. **15** (12), 3715–3727 (2006).

[7] Motohashi S., Nagata T., Goto T., Aoki R., Chen H. A study on blind image restoration of blurred images using R-map. 2018 International Workshop on Advanced Image Technology (IWAIT). 1–4 (2018).

[8] Rudin L., Osher S., Fatemi E. Non linear total variation based noise removal algorithms. Physica D. **60** (1–4), 259–268 (1996).

[9] Chan T. F., Wong C.-K. Total variation blind deconvolution. IEEE Transactions on Image Processing. **7** (3), 370–375 (1998).

[10] Semmane F. Z., Moussaid N., Ziani M. Searching for similar images using Nash game and machine learning. Mathematical Modeling and Computing. **11** (1), 239–249 (2024).

[11] Salah F.-E., Moussaid N. Machine learning and similar image-based techniques based on Nash game theory. Mathematical Modeling and Computing. **11** (1), 120–133 (2024).

[12] Elmoumen S., Moussaid N., Aboulaich R. Image retrieval using Nash equilibrium and Kalai–Smorodinsky solution. Mathematical Modeling and Computing. **8** (4), 646–657 (2021).

[13] Meskine D., Moussaid N., Berhich S. Blind image deblurring by game theory. NISS'19: Proceedings of the 2nd International Conference on Networking, Information Systems & Security. 31 (2019).

[14] Alaa K., Atounti M., Zirhem M. Image restoration and contrast enhancement based on a nonlinear reaction-diffusion mathematical model and divide and conquer technique. Mathematical Modeling and Computing. **8** (3), 549–559 (2021).

[15] Alaa H., Alaa N. E., Aqel F., Lefraich H. A new Lattice Boltzmann method for a Gray–Scott based model applied to image restoration and contrast enhancement. Mathematical Modeling and Computing. **9** (2), 187–202 (2022).

[16] Ross B. A brief history and exposition of the fundamental theory of fractional calculus. Fractional Calculus and Its Applications. Lecture Notes in Mathematics. Vol. 457, 1–36 (2006).

[17] Loverro A. Fractional Calculus: History, Definitions and Applications for the Engineer. University of Notre Dame: Department of Aerospace and Mechanical Engineering (2004).

[18] Liu S.-C., Chang S. Dimension estimation of discrete-time fractional Brownian motion with applications to image texture classification. IEEE Transactions on Image Processing. **6** (8), 1176–1184 (1997).

[19] Ninness B. Estimation of 1/f noise. IEEE Transactions on Information Theory. **44** (1), 32–46 (1998).

[20] Engheta N. On the role of fractional calculus in electromagnetic theory. IEEE Antennas and Propagation Magazine. **39** (4), 35–46 (1997).

[21] Unser M. Splines: A perfect fit for signal and image processing. IEEE Signal Processing Magazine. **16** (6), 22–38 (1999).

[22] Unser M., Blu T. Fractional splines and wavelets. SIAM Review. **42** (1), 43–67 (2000).

[23] Aboulaich R., Habbal A., Moussaid N. Optimisation multicritère: une approche par partage des variables. ARIMA. **13**, 77–89 (2010).

[24] Wang Z., Bovik A. C., Sheikh H. R., Simoncelli E. P. Image quality assessment: from error visibility to structural similarity. IEEE Transactions on Image Processing. **13** (4), 600–612 (2004).

До підходу ігрової стратегії Неша до сліпої деконволюції зображення: варіаційна структура похідної дробового порядку

Салах Ф.-Е.[1], Муссаїд Н.[1], Абасі А.[1], Джадір А.[2]

[1]*LMCSA, FSTM, Університет Хасана II Касабланки, Мохаммедія, Марокко*
[2]*FSTG, Університет Каді Айяда, Марракеш, Марокко*

Відновлення зображень — це критично важливий процес, спрямований на відновлення пошкоджених зображень, на які часто впливають такі фактори, як розмиття від руху, розмиття датчика, розфокусована фотографія, оптичні аберації, атмосферні спотворення та розмиття, спричинене шумом. Внутрішня проблема полягає в типовому сценарії, коли невідомі ні оригінальне зображення, ні ядро розмиття (функція розповсюдження точки, PSF). Цей відновлювальний процес знаходить застосування в різних сферах, включаючи зондування, медичну візуалізацію, астрономію, дистанційне зондування та кримінальні розслідування. Ця стаття представляє інноваційний підхід до сліпої деконволюції зображення на основі теорії ігор Неша. Наша увага зосереджена на відновленні лінійно пошкоджених зображень без обробки явних знань про вихідне зображення чи ядро розмиття (PSF). Запропонований метод формулює сліпу деконволюцію як статичну гру для двох гравців, де один гравець займається видаленням розмиття зображення, а інший зосереджений на оцінці PSF. Оптимальний розв'язок характеризується як рівновага Неша, що призводить до ефективного відновлення зображення. Крім того, представлено розширене формулювання гри, яка включає похідні дробового порядку. Це нове розширення має потенціал для підвищення точності та надійності відновлення зображень, сприяючи прогресу в області сліпої деконволюції зображень та її практичного застосування.

Ключові слова: *сліпа деконволюція; реставрація; багатокритеріальна оптимізація; похідна дробового порядку; рівновага Неша.*